Contribution from the J. Tuzo Wilson Laboratories, Erindale College, University of Toronto, Mississauga, Ontario, Canada L5L 1C6

Kinetics of Reaction of Bis(diphenylphosphino)methane with Dodecacarbonyltriruthenium

BIMLA AMBWANI, SUDHIR CHAWLA, and ANTHONY POË*

Received July 2, 1984

Reaction of dppm ($Ph_2PCH_2PPh_2$) with $Ru_3(CO)_{12}$ proceeds via the complexes $Ru_3(CO)_{10}(\mu$-dppm) and $Ru_3(CO)_9(\mu$-dppm)(η^1-dppm) to form the very stable $Ru_3(CO)_8(\mu$-dppm)$_2$, and the kinetics of the three reactions in benzene have been followed. Reaction with $Ru_3(CO)_{12}$ proceeds mainly by a ligand-dependent path, and dppm is about twice as nucleophilic as PPh_3 toward this cluster. $Ru_3(CO)_{10}(\mu$-dppm) reacts with dppm to form $Ru_3(CO)_9(\mu$-dppm)(η^1-dppm) by two paths. The main path (ca. 80%) follows kinetics characteristic of a reversible CO dissociative path. The minor path is completely inhibited by CO, even at high [dppm], and may involve dissociation of CO from an already substituted Ru atom before transfer of the unsaturation to the $Ru(CO)_4$ moiety. The bridge formation reaction undergone by $Ru_3(CO)_9(\mu$-dppm)(η^1-dppm) to give the final product also occurs via two paths, but in this case they are of approximately equal importance. One is not affected by CO and is assigned to dissociative loss of CO from a bridged Ru atom, formation of the second bridge following very rapidly. The other may involve reversible loss of CO from the $Ru(CO)_3(\eta^1$-dppm) moiety followed by transfer of the unsaturation to one of the other Ru atoms.

Introduction

Metal carbonyl clusters containing bridging ligands are of interest since the bridging ligands may be capable of stabilizing the clusters against fragmentation without preventing formation of reactive, and potentially catalytic, species by such processes as metal–metal bond homolysis.[1] In spite of this there have been no quantitative kinetic studies of their stabilities toward fragmentation or substitution, and no comparison is therefore possible at the moment with analogous clusters substituted with monodentate ligands. Both the stereochemical disposition of the substituting donor atoms and the effects of their coordination on the rest of the cluster are likely to be different with bridging than with monodentate ligands. Since it seems probable that this will have kinetic and mechanistic effects, we have begun a series of kinetic studies of clusters containing such ligands. We report here the kinetics of the reactions involved in the formation of $Ru_3(CO)_8(\mu$-dppm)$_2$ by thermal reaction of dppm with $Ru_3(CO)_{12}$. The synthesis and structure of $Ru_3(CO)_8(\mu$-dppm)$_2$ have been reported,[2] and the two dppm ligands are both bridging, the P atoms occupying equatorial positions around the Ru_3 cluster. The structure of $Ru_3(CO)_{10}(\mu$-dppm) has also been reported and discussed in detail.[3]

Experimental Section

Preparation of Complexes. $Ru_3(CO)_{12}$ and dppm were obtained from Strem Chemicals and used as received. $Ru_3(CO)_{10}(\mu$-dppm) was prepared by reaction of $Ru_3(CO)_{12}$ (320 mg, 0.50 mmol) with dppm (210 mg, 0.54 mmol) in dry THF (50 mL). Solutions were degassed in a Schlenk tube and left under vacuum at room temperature for 48 h. Reduction of volume, elution from a Fluorosil column with THF–hexane (3:1), evaporation to dryness, and precipitation from dichloromethane by addition of *n*-hexane led to good yields of orange-red crystals of $Ru_3(CO)_{10}(\mu$-dppm). Anal. Calcd: C, 43.43; H, 2.28. Found: C, 43.58; H, 2.49. The IR spectrum in 1,2-dichloroethane was measured with a Perkin-Elmer 298 spectrophotometer (ν(CO)): 2080 (m), 2040 (vw), 2010 (s), 1960 (w) cm^{-1}. Cf. IR in (ν(CO)) in CH_2Cl_2: 2080 (m), 2040 (w), 2010 (s), 1960 (m) cm^{-1}.[4] The UV–vis spectrum in benzene was measured with a Cary 210 spectrophotometer and showed a band at 424 nm (ϵ, 8.3×10^3 M^{-1} cm^{-1}).

$Ru_3(CO)_8(\mu$-dppm)$_2$ was prepared by reacting $Ru_3(CO)_{12}$ (200 mg, 0.3 mmol) with dppm (400 mg, 1.2 mmol) in dry, degassed THF (50 mL) at 60 °C for 6 h. Purification and recrystallization as for $Ru_3(CO)_{10}(\mu$-dppm) led to good yields of orange crystals of $Ru_3(CO)_8(\mu$-dppm)$_2$. Anal. Calcd: C, 53.75; H, 3.40; P, 9.58. Found: C, 53.28; H, 3.14; P, 9.05. IR in $C_2H_4Cl_2$: 2040 (m), 1967 (s), 1900 (w) cm^{-1}. Cf. IR in CsBr pellets: 2040 (s), 1955 (br), 1890 (m) cm^{-1}.[2a] λ_{max} in benzene: 435 nm (ϵ, 1.1×10^4 M^{-1} cm^{-1}.)

Kinetics. The kinetics were followed by monitoring changes in the electronic spectra of solutions placed in thermostated cell holders of a Cary 16K or Cary 210 spectrophotometer. Temperatures of reacting solutions were measured with a Minco platinum resistance thermometer and were constant to within ±0.1 °C. Slower reactions were monitored by repetitive scanning and faster ones by absorbance measurements at a single wavelength by using the continuous drive mode. Pseudo-first-order rate constants were obtained graphically, and the dependence on [dppm], [CO], and temperature was analyzed by suitably weighted least-squares techniques where necessary.

Results and Discussion

Course of the Reactions. The reaction of $Ru_3(CO)_{10}(\mu$-dppm) with dppm in benzene at 30–70 °C proceeds to form $Ru_3(CO)_8(\mu$-dppm)$_2$ in two stages. The first is accompanied by the replacement of the band at 424 nm due to the reactant by one at 450 nm that is ca. 25% more intense. This is subsequently replaced by the band at 435 nm, characteristic of $Ru_3(CO)_8(\mu$-dppm)$_2$, that is ca. 10% less intense than that at 450 nm due to the intermediate. This results in a growth of absorbance at 450 nm during the first stage, followed by a decrease during the second stage of reaction. At lower temperatures and under an atmosphere of CO, the first stage shows isosbestic points at 398 and 420 nm due to a slight overlap of the spectra of $Ru_3(CO)_{10}(\mu$-dppm) and the product of the first stage (Figure 1A). When the temperature is increased, or when the reactions are carried out under argon or air, the absorption below 450 nm at the end of the first stage is significantly higher so that the spectra of the original complex and the product or products of the first stage do not overlap. There are, therefore, no isosbestic points shown during reactions under these conditions. The spectral changes during the first stage are very similar to those seen during reaction with PPh_3 to form $Ru_3(CO)_9(\mu$-dppm)(PPh_3), when a new maximum grows at 460 nm with an intensity 20% greater than that of the reactant at 424 nm.[5]

The spectroscopic changes during the second stage show a sharp isosbestic point at 428 nm when the reaction is carried out at lower temperatures and under CO (Figure 1B). When it is carried out under Ar or at higher temperatures, the absorption of the final product or products at lower wavelengths is somewhat greater and the isobestic point, while still quite sharp, moves up to 435 nm.

When reactions were carried out in 1,2-dichloroethane at temperatures between 30 and 60 °C, the first stage was accompanied by the formation of the intermediate product with bands at 2080 (m), 2000 (s), and 1980 (s, br) cm^{-1}. The second stage leads to the spectrum characteristic of isolated $Ru_3(CO)_8(\mu$-dppm)$_2$, which remains unchanged for at least 24 h at 40 °C. The spectral changes during the first stage are virtually identical with those seen during reaction with PPh_3 over the same time period with the exception that the product of that reaction has a negligible absorbance at 2080 cm^{-1}.[5]

Thus, reaction with dppm leads first to a product with IR and UV–vis spectra very similar to those observed after reaction with the monodentate ligand PPh_3, and this is followed by reaction to form the dibridged complex $Ru_3(CO)_8(\mu$-dppm)$_2$. The initial

(1) E.g.: Bahsoun, A. A.; Osborne, J. A.; Voekler, C.; Bonnet, J. J.; Lavigne, G. *Organometallics* **1982**, *1*, 1114.
(2) (a) Lavigne, G.; Bonnet, J. J. *Inorg. Chem.* **1981**, *20*, 2713. (b) Lavigne, G.; Lugan, N.; Bonnet, J. J. *Acta Crystallogr., Sect. B: Struct. Crystallogr. Cryst. Chem.* **1982**, *38B*, 1911.
(3) Coleman, A. W.; Jones, D. F.; Dixneuf, P. H.; Brisson, C.; Bonnet, J. J.; Lavigne, G. *Inorg. Chem.* **1984**, *23*, 952.
(4) Cotton, F. A.; Hanson, B. E. *Inorg. Chem.* **1977**, *16*, 3369.
(5) Ambwani, B.; Chawla, S. K.; Poë, A. J., unpublished observations.

0020-1669/85/1324-2635$01.50/0

substitution by the dppm or PPh_3 must occur at the unsubstituted Ru atom in $Ru_3(CO)_{10}(\mu$-dppm) to form a trisubstituted cluster with one P-donor substituent atom on each Ru atom. No evidence exists for disubstitution by P-donor ligands on one Ru atom in a Ru_3 cluster unless all other Ru atoms are singly substituted. Disubstitution on a single metal in such complexes only occurs for small ligands such as $P(OMe)_3$[6] or with bridging ligands such as dppm.[2b] The spectroscopic evidence leaves little doubt, therefore, that the product of the first stage is $Ru_3(CO)_9(\mu$-dppm$)(\eta^1$-dppm) in which each Ru atom has a P-donor atom attached to it. The second stage must therefore involve intramolecular bridge formation to give the known product $Ru_3(CO)_8(\mu$-dppm$)_2$. Once formed, $Ru_3(CO)_8(\mu$-dppm$)_2$ is very stable.

Changes in the UV–vis spectra show that reaction of $Ru_3(CO)_{12}$ with dppm proceeds to $Ru_3(CO)_9(\mu$-dppm$)(\eta^1$-dppm), which then reacts more slowly to form $Ru_3(CO)_8(\mu$-dppm$)_2$. Spectroscopic changes over the first part of the reaction vary with [dppm]. This is likely to be due to the accumulation of different concentrations of intermediates during formation of $Ru_3(CO)_9(\mu$-dppm$)(\eta^1$-dppm). The reaction sequence to form this complex is most probably as shown in eq 1–3, reaction 4 then leading to the final

$$Ru_3(CO)_{12} + \text{dppm} \rightarrow Ru_3(CO)_{11}(\eta^1\text{-dppm}) + CO \quad (1)$$

$$Ru_3(CO)_{11}(\eta^1\text{-dppm}) \rightarrow Ru_3(CO)_{10}(\mu\text{-dppm}) + CO \quad (2)$$

$$Ru_3(CO)_{10}(\mu\text{-dppm}) + \text{dppm} \rightarrow Ru_3(CO)_9(\mu\text{-dppm})(\eta^1\text{-dppm}) + CO \quad (3)$$

$$Ru_3(CO)_9(\mu\text{-dppm})(\eta^1\text{-dppm}) \rightarrow Ru_3(CO)_8(\mu\text{-dppm})_2 + CO \quad (4)$$

product. The proposed initial product is analogous to $Ru_3(CO)_{11}(\eta^1$-dppe) (dppe = $Ph_2PCH_2CH_2PPh_2$), which has been characterized by Bruce et al.[7] Bridge closure of this complex to form $Ru_3(CO)_{10}(\mu$-dppe) is quite slow and reaction 2 may be comparably slow. As will be seen below, reaction 1 is first order in [dppm] whereas reaction 2 is virtually certain to be independent of [dppm],[8] as is reaction 3. Reaction 1 varies from being somewhat slower than reaction 3 at low [dppm] to being considerably faster at higher [dppm]. It is not surprising, therefore, that the spectroscopic changes should be dependent on [dppm].

Kinetics of Reaction of $Ru_3(CO)_{12}$. Although the spectroscopic changes vary with [dppm] and are likely to reflect different accumulations of the intermediates $Ru_3(CO)_{11}(\eta^1$-dppm) and $Ru_3(CO)_{10}(\mu$-dppm), it is still possible to obtain meaningful rate constants. Thus, at 40 °C and low [dppm] there is an isosbestic point at 400 nm over much of the reaction, and Swinbourne plots[9] of data during the existence of these points were quite linear. On the other hand, at higher [dppm], absorbances at some wavelengths rose steadily to an approximately constant value so that A_∞ values were reasonably well-defined, and quite good plots of log $(A_\infty - A_t)$ against t were obtained. The dependence of k_{obsd} on [dppm] is plotted in Figure 2. Over the concentration range used the reaction is essentially first order in [dppm] with a second-order rate constant of 2.4×10^{-3} M^{-1} s^{-1}. Reaction with PPh_3 suggests[10] that there must also be a [dppm]-independent path with a rate constant of 0.11×10^{-4} s^{-1}, but the data are not precise enough to detect this. The value of k_2 shows that, at 40 °C, dppm is about twice as nucleophilic as PPh_3[10] toward $Ru_3(CO)_{12}$, allowing for the fact that each dppm has two nucleophilic P atoms. On the other hand, PPh_2Me is ca. 20 times more nucleophilic than PPh_3 at 60 °C.[11] These data are in agreement with the expectation that a CH_2PPh_2 group attached to PPh_2 would enhance the basicity of the P atom in the latter less than a CH_3 group and also lead to larger unfavorable steric effects.

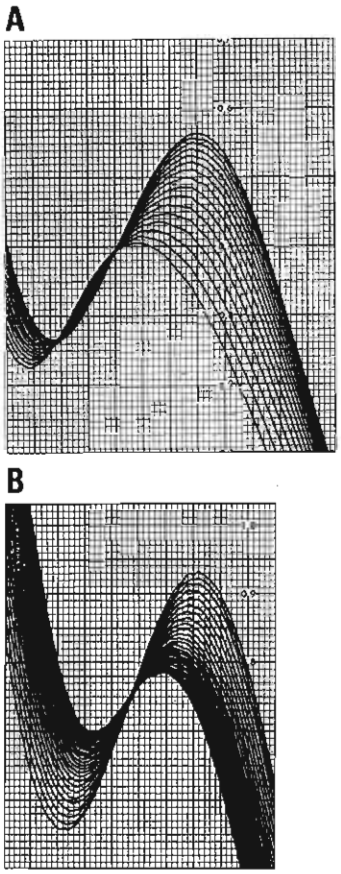

Figure 1. Changes in the UV–vis spectra during the reaction of $Ru_3(CO)_{10}(\mu$-dppm) with dppm under CO at 40 °C: (A) growth of an absorption maximum at 450 nm during the first stage of reaction, with isosbestic points at 398 and 420 nm; (B) the decrease of the maximum at 450 nm during the second stage and its replacement by one at 435 nm due to the final product, $Ru_3(CO)_8(\mu$-dppm$)_2$. These spectra were run with absorbance suppression of 0.2 and absorbance range of 0.5.

Table I. First-Order Rate Constants for Reaction of $Ru_3(CO)_{10}(\mu$-dppm) with dppm in Benzene

T, °C	[dppm], M	$10^4 k_{av}$,[a] s^{-1}
30.0	0.01	0.501 ± 0.013
35.0	0.01	1.08 ± 0.05
40.0	0.001–0.248	1.85 ± 0.04 (1.95 ± 0.09)
50.0	0.001–0.248	8.09 ± 0.13 (7.39 ± 0.35)
60.0	0.001–0.248	22.3 ± 0.6 (22.8 ● 1.0)
70.0	0.248	72.8 ± 2.4 (70.7 ± 3.3)

[a] The rate constants are generally the average of a substantial number of independent measurements corrected, in some cases, for small differences in temperature according to the activation enthalpy quoted in Table II. The probable error (standard deviation) estimated by the method of pooled variances for an individual measurement at any temperature is ±6.7%. Data are for reactions under air or argon or (in parentheses) for reactions only under argon.

Kinetics of Reactions of $Ru_3(CO)_{10}(\mu$-dppm). Values of the rate constants are summarized in Table I. Reactions under air proceed at rates independent of [dppm] from 0.001 to 0.25 M. Rates under Ar are the same as under air, and the reactions are therefore unaffected by the presence of O_2. Thus reactions under Ar are 5.4% higher, 8.7% lower, 2.2% higher, and 2.9% lower than

(6) Benfield, R. E.; Johnson, B. F. G. *Transition Met. Chem. (Weinheim, Ger.)* **1981**, *6*, 131.
(7) Bruce, M. I.; Hambley, T. W.; Nicholson, B. K.; Snow, M. R. *J. Organomet. Chem.* **1982**, *235*, 83.
(8) Sekhar, V. C.; Poë, A. J. *J. Am. Chem. Soc.* **1984**, *106*, 5034.
(9) Swinbourne, E. S. "Analysis of Kinetic Data"; Nelson: London, 1971; p 81.
(10) Poë, A. J.; Twigg, M. V. *J. Chem. Soc., Dalton Trans.* **1974**, *1860*.
(11) Twigg, M. V. *Inorg. Chim. Acta* **1977**, *21*, L7.
(12) Wilhelm, E.; Battino, R. *Chem. Rev.* **1973**, *73*, 1.

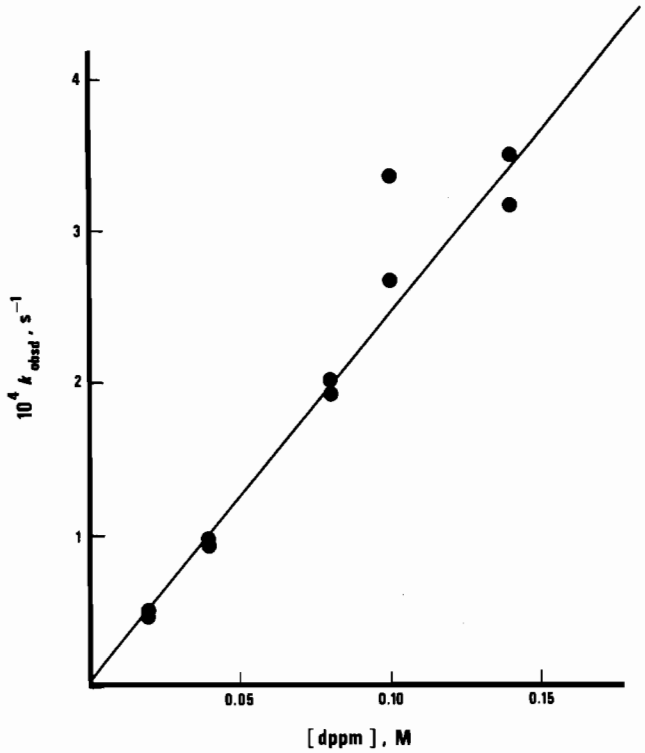

Figure 2. Dependence of k_{obsd} on [dppm] for the reaction of dppm with $Ru_3(CO)_{12}$ in benzene at 40 °C.

Table II. Activation Parameters[a] for Reactions Specified

reacn	$\Delta H^{\ddagger}$, kcal mol^{-1}	$\Delta S^{\ddagger}$, cal K^{-1} mol^{-1}
$Ru_3(CO)_{10}(\mu\text{-dppm})$ + dppm (under air or Ar)	24.96 ± 0.51	+4.2 ± 1.7
$Ru_3(CO)_9(\mu\text{-dppm})(\eta^1\text{-dppm}) \rightarrow Ru_3(CO)_8(\mu\text{-dppm})_2$	30.97 ± 0.43[b]	+18.0 ± 1.32[b]
$Ru_3(CO)_9(\mu\text{-dppm})(\eta^1\text{-dppm}) \rightarrow Ru_3(CO)_8(\mu\text{-dppm})_2$	24.46 ± 0.44[c]	−1.62 ± 1.35[c]

[a] Uncertainties are probable errors. [b] Reaction not inhibited by CO. [c] Reaction completely inhibited by CO. Rate constants for this reaction were estimated by subtracting those for reaction under CO from those under air or argon. (See Table III.)

the average of all values at 40, 50, 60, and 70 °C, respectively. The dependence of the rate constants on temperature leads to the activation parameters shown in Table II. Reactions are retarded by CO, and the dependence of k_{obsd} on [dppm] under an atmosphere of CO is shown in Figure 3. This suggests that the reaction proceeds by a reversible CO dissociative mechanism as shown in eq 5 and 6 for which the rate equation would be as shown in (7).

$$Ru_3(CO)_{10}(\mu\text{-dppm}) \underset{k_{-5}}{\overset{k_5}{\rightleftharpoons}} Ru_3(CO)_9(\mu\text{-dppm}) + CO \quad (5)$$

$$Ru_3(CO)_9(\mu\text{-dppm}) + dppm \xrightarrow{k_6} Ru_3(CO)_9(\mu\text{-dppm})(\eta^1\text{-dppm}) \quad (6)$$

$$k_{obsd} = (k_5k_6[dppm]/k_{-5}[CO])/(1 + k_6[dppm]/k_{-5}[CO]) \quad (7)$$

A weighted least-squares analysis of the dependence of $1/k_{obsd}$ on [CO]/[dppm] at 50.7 °C leads to the values $k_5 = (6.95 \pm 0.10) \times 10^{-4}$ s^{-1} and $k_6/k_{-5} = 0.124 \pm 0.005$, the standard deviation, $\sigma(k_{obsd})$, of an individual determination of k_{obsd} being ±6.1%. The value of k_5 is significantly lower than that for k_{obsd} found under air or Ar, a value of $(8.84 \pm 0.14) \times 10^{-4}$ s^{-1} being calculated by using the activation parameters in Table II and another of $(9.09 \pm 0.20) \times 10^{-4}$ s^{-1} being calculated by adjusting 10 values of k_{obsd} measured at 50.0–50.5 °C according to the activation enthalpy and averaging them. These values lead to the ratios 1.27 ± 0.03 and 1.31 ± 0.03, respectively, for the ratio of the limiting rate constant under air or argon to that under CO. This phenomenon

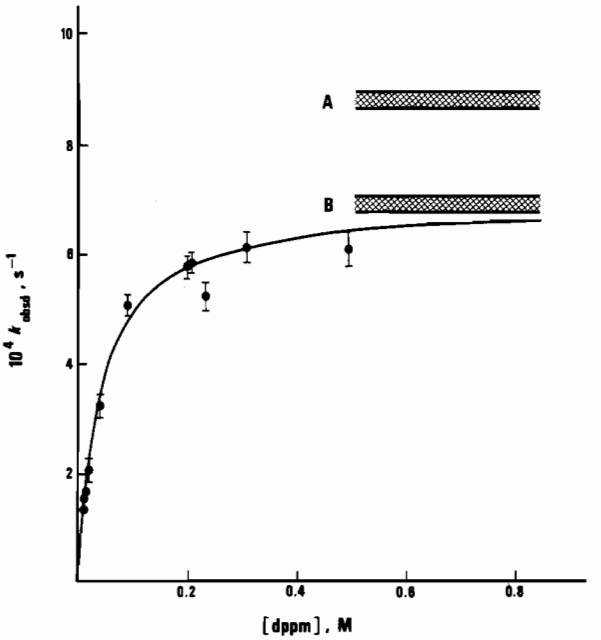

Figure 3. Dependence of k_{obsd} on [dppm] for the reaction of dppm with $Ru_3(CO)_{10}(\mu\text{-dppm})$ under 1 atm of CO at 50.7 °C. The line drawn through the data is calculated according to the parameters obtained by a weighted linear-least-squares analysis of the dependence of 25 values of $1/k_{obsd}$ on [CO]/[dppm] where [CO] is taken as 5.4×10^{-3} M.[12] A indicates the limiting rate for reactions under air or argon (calculated from the activation parameters), and B indicates the limiting rate for reaction under CO, the crosshatching indicating the probable error of these limiting values.

Scheme I

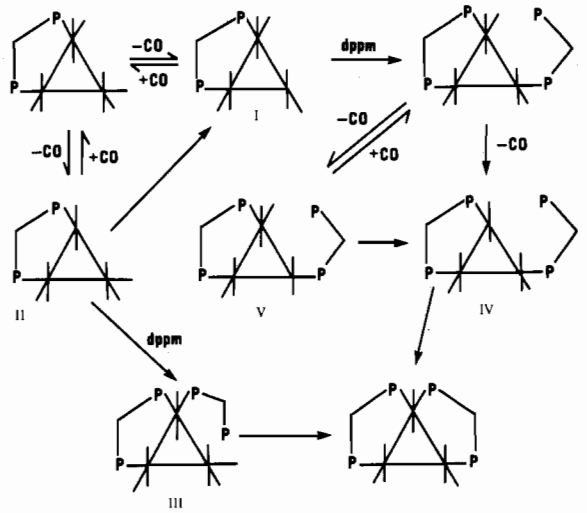

was confirmed by carrying out reactions simultaneously under argon and under CO with [dppm] = 0.23–0.25 M. These values of [dppm] were not quite sufficient to bring about limiting rates under CO, but a correction factor of 1.19 can be derived from the value of k_6/k_{-5} given above. After this correction, ratios of 1.34, 1.30, 1.20, and 1.31 were found, respectively, at 40.0, 50.0, 60.5, and 69.6 °C, in good agreement with those listed above. The absence of any clear dependence of this ratio on temperature suggests that the value of $\Delta H^{\ddagger}$ for the reaction under CO is not very different from the value given in Table II.

These kinetic data, combined with the spectroscopic results described above, suggest that reaction occurs by two paths. The major one accounts for 80% of the reaction under air or argon and shows kinetic behavior entirely consistent with reversible dissociation of a CO from the $Ru(CO)_4$ moiety. The coordinatively unsatured $Ru(CO)_3$ moiety is then competitively attacked either by CO or by dppm to form $Ru_3(CO)_9(\mu\text{-dppm})(\eta^1\text{-dppm})$ as shown in Scheme I. The nature of the minor path is not certain,

Table III. Rate Constants[a] for the Reaction $Ru_3(CO)_9(\mu\text{-dppm})(\eta^1\text{-dppm}) \rightarrow Ru_3(CO)_8(\mu\text{-dppm})_2 + CO$ in Benzene

T, °C	[dppm], M	$10^5 k_{av}$,[b] s^{-1}	$10^5 k_{av}$,[c] s^{-1}
31.0	0.001	0.93 ± 0.07	
41.0	0.001–0.240	4.42 ± 0.10	1.45 ± 0.07
		(4.18 ± 0.17)	
50.0	0.001–0.233	15.4 ± 0.24	6.98 ± 0.22
		(15.6 ± 0.54)	(6.56 ± 0.33)
60.0	0.01–0.232	55.5 ± 1.0	28.5 ± 1.4
		(54.7 ± 2.7)	(34.6 ± 1.7)
70.0	0.236	195 ± 7	109 ± 5
		(194 ± 10)	

[a] Values are averages as described in footnote *a*, Table I. [b] For all reactions under air or argon or (in parentheses) for reactions only under Ar. [c] For reactions under 100% CO or (in parentheses) under 41% CO in $CO-N_2$ mixtures.

but an attractive possibility is also shown in Scheme I. Dissociative loss of CO from an already substituted Ru atom leads to II. The vacant coordination site in II is susceptible to attack by CO but is not at all, or only very weakly, susceptible to attack by dppm for steric reasons. In the absence of CO, the coordinative unsaturation can be transferred to the unsubstituted Ru atom, by CO migration in the opposite direction, with formation of I. This transfer of unsaturation must be slower than reattachment of CO to II when reactions are carried out under CO. If dppm were to add to II to form III, III would then be expected to form $Ru_3(CO)_8(\mu\text{-dppm})_2$ very rapidly. The IR spectra show that this does not occur to any detectable extent, but the slightly different changes in the UV–vis spectra (observed when reactions are carried out under air rather than CO or at higher temperatures) do suggest that II is capable of forming a side product in small amounts under some conditions. This type of mechanism has been proposed previously[13] by Sonnenberger and Atwood, though we believe that this is the first kinetic evidence consistent with such a sequence of reactions.

Kinetics of Reaction of $Ru_3(CO)_9(\mu\text{-dppm})(\eta^1\text{-dppm})$. This complex reacts to form $Ru_3(CO)_8(\mu\text{-dppm})_2$, and reaction therefore involves intramolecular bridge formation by the initially monodentate dppm ligand. Values of the rate constants are summarized in Table III. These show that the reaction proceeds by two paths of approximately equal importance, neither of which is affected by [dppm]. One is completely inhibited by CO, and the other is not inhibited at all. Thus the depression of the rate is the same, or very nearly the same, under 41% CO as under 100% CO. The path inhibited by CO is accompanied by slightly different changes in the UV–vis spectra, but any side product formed is not produced in sufficient amounts to be detectable in the IR spectra. The activation parameters for the two paths are shown in Table II. The path that is not retarded by CO has parameters clearly characteristic of a dissociative mechanism. This path most probably involves dissociation of an equatorial CO from a Ru atom that is already bridged by a dppm ligand to form IV as shown in Scheme I. The vacant coordination site in IV is exactly where the free end of the monodentate dppm has to enter to form the thermodynamically favored product. Even in the presence of CO, this intramolecular reaction should be much faster than the bimolecular recoordination of a free CO ligand because of the high local concentration of the free end of the monodentate dppm.[14] Although CO dissociative in nature, this path is, therefore, *not* retarded by CO.

The path that is inhibited by CO could involve dissociation of a CO from a different position in the molecule, one that is not favorable for immediate attack by the free end of the dppm. This could be an axial CO on a bridged Ru atom or, more probably, an axial or equatorial CO on the Ru ligated by monodentate dppm. The last possibility, shown in Scheme I, would lead to intermediate V. Recoordination of CO, if it is present, competes successfully with transfer of the vacant coordination site (by CO migration) to form IV. This transfer does occur in the absence of CO, so leading to a faster overall reaction. V might also be capable of reacting to form a side product in small amounts, so accounting for the slightly different changes in the UV–vis spectra observed for reactions under air rather than under CO. It is interesting that the rate of reaction by this path at 50 °C is $(0.84 \pm 0.03) \times 10^{-4}$ s^{-1} as compared with a rate of $(0.9 \pm 0.1) \times 10^{-4}$ s^{-1} for the correspondingly assigned path for $Ru_3(CO)_{10}(\mu\text{-dppm})$, allowing for the fact that two Ru atoms are available for the latter reaction and one one for the former. Similarly the latter rate constant can be compared with a value of $(0.70 \pm 0.02) \times 10^{-4}$ s^{-1} assigned to dissociation from a bridged Ru atom in $Ru_3(CO)_9(\mu\text{-dppm})(\eta^1\text{-dppm})$. In this case the statistical factor has not been applied. The equatorial position assigned to the η^1-dppm in this complex only allows dissociation from *one* of the bridged Ru atoms to be easily followed by formation of the second bridge. Even without these statistical adjustments the rate constants assigned to CO loss from a ligated Ru atom are remarkably close in the two complexes.

The activation parameters for the path completely inhibited by CO (Table II) are not incompatible with CO dissociation of the type suggested although the value of $\Delta S^\ddagger$ is small and not positive as one might expect. However, even quite strongly negative values of $\Delta S^\ddagger$ have been observed[15] for reactions of clusters that are inhibited by CO. These were explained by more complex formulations of the coordinatively unsaturated intermediate than is indicated by V in Scheme I, and a similar explanation can be invoked here.

The dissociative nature of both paths for the intramolecular bridge formation reaction is in striking contrast with the only other such reaction that has been studied.[8] Thus the absence of CO inhibition and the activation parameters $\Delta H^\ddagger = 22.22 \pm 0.44$ kcal mol^{-1} and $\Delta S^\ddagger = -9.6 \pm 1.3$ cal K^{-1} mol^{-1} for reaction 8 are only

$$Os_3(CO)_{11}(\eta^1\text{-dppm}) \rightarrow Os_3(CO)_{10}(\mu\text{-dppm}) + CO \quad (8)$$

compatible with an intramolecular S_N2 mechanism.[8] This difference can be ascribed to the substituted nature of the Ru atom. Associative substitution at a metal atom is greatly retarded if a substituent is already present on that metal.[16]

Acknowledgment. We thank the Natural Sciences and Engineering Research Council and Erindale College for support.

Registry No. dppm, 2071-20-7; $Ru_3(CO)_{12}$, 15243-33-1; $Ru_3(CO)_{10}(\mu\text{-dppm})$, 64364-79-0; $Ru_3(CO)_9(\mu\text{-dppm})(\eta\text{-dppm})$, 97042-90-5.

Supplementary Material Available: Table of constants for reaction of $Ru_3(CO)_{10}(\mu\text{-dppm})$ with dppm under CO (1 page). Ordering information is given on any current masthead page.

(13) Sonnenberger, D.; Atwood, J. D. *J. Am. Chem. Soc.* **1980**, *102*, 3484; **1982**, *104*, 2113; *Organometallics* **1982**, *1*, 694.

(14) Basolo, F.; Pearson, R. G. "Mechanisms of Inorganic Reactions"; Wiley: New York, 1967; p 225.

(15) Malik, S. K.; Poë, A. J. *Inorg. Chem.* **1979**, *18*, 1241.

(16) Howell, J. A. S.; Burkinshaw, P. M. *Chem. Rev.* **1983**, *83*, 557.